Vol 17 No 3, March 2008
1674-1056/2008/17(03)/0995-05
Chinese Physics B
© 2008 Chin. Phys. Soc.
and IOP Publishing Ltd

Polarization dependent dispersion and its impact on optical parametric process in high nonlinear microstructure fibre*

Xiao Li(肖 礼)†, Zhang Wei(张 巍),
Huang Yi-Dong(黄翊东), and Peng Jiang-De(彭江得)

Department of Electronic Engineering, Tsinghua University, Beijing 100084, *China*

(Received 12 July 2007; revised manuscript received 27 July 2007)

High nonlinear microstructure fibre (HNMF) is preferred in nonlinear fibre optics, especially in the applications of optical parametric effects, due to its high optical nonlinear coefficient. However, polarization dependent dispersion will impact the nonlinear optical parametric process in HNMFs. In this paper, modulation instability (MI) method is used to measure the polarization dependent dispersion of a piece of commercial HNMF, including the group velocity dispersion, the dispersion slope, the fourth-order dispersion and group birefringence. It also experimentally demonstrates the impact of the polarization dependent dispersion on the continuous wave supercontinuum (SC) generation. On one axis MI sidebands with symmetric frequency detunings are generated, while on the other axis with larger MI frequency detuning, SC is generated by soliton self-frequency shift.

Keywords: microstructure fibre, modulation instability, dispersion, birefringence
PACC: 4265, 4281

1. Introduction

High nonlinear microstructure fibre (HNMF), which has a silica core and complex cladding composed of periodical air pillars in silica background, has shown its great potential in applications of fibre nonlinear optics.[1,2] Due to the small core size and high air filled fraction of holey cladding, stronger light confinement is achieved in HNMFs, comparing with traditional single mode fibres. On the other hand, complex structure in the cladding provides the flexibility in fibre dispersion design, which is preferred in many nonlinear applications needing phase matching.[3] Many applications have been explored based on HNMFs, such as supercontinuum (SC) generation,[4,5] photon pair generation,[6] broadband parametric amplification,[7] wavelength conversion[8] etc. Recently, it has been proposed that HNMF in telecom bandwidth shows intrinsic high birefringence, even splitting of zero dispersion wavelengths (ZDWs) along two axes, due to the asymmetries induced during fabrication.[9] However, the difficulty in dispersion measurement of the short HNMF sample near the ZDWs limits the study of its polarization dependent dispersion properties. The impacts of the polarization dependent dispersion on the nonlinear effects in HNMFs have not been explored comprehensively yet.

In our previous work, we demonstrated that ultrahigh parametric amplification gain efficiency can be achieved in a piece of HNMF.[10] However, its dispersion properties have not been studied. In this paper, we modify the modulation instability (MI) method,[11] which was proposed to measure the dispersion properties of the traditional high nonlinear fibre, by considering the pump polarization. Using the modified MI method, we measure the polarization dependent dispersion properties of the HNMF sample, including the group velocity dispersion, the dispersion slope, the fourth-order dispersion and group birefringence. The impact of polarization dependent dispersion properties on the parametric process near the ZDWs in the HNMF is also demonstrated experimentally.

This paper is structured as follows. The method and experimental setup of the dispersion measurement by MI method are introduced in Section 2. The measurement results of various dispersion parameters are presented in Section 3, including: phase birefringence, polarization dependent group velocity dispersions (GVDs) and their slopes, the fourth-order dispersion, and group velocity birefringence. In Section

*Project supported by the National Basic Research Program (973 Program) of China (Grant No 2003CB314904).
†Corresponding author. E-mail: xiaoli99@mails.thu.edu.cn

4, the impact of the polarization dependent dispersion on the parametric process is demonstrated experimentally. Section 5 is the conclusion.

2. Method and experimental setup

The MI method for measuring the fibre GVD parameters bases on the physical process of amplified spontaneous parametric emission spectrum. When an intensive light is injected into the fibre in the anomalous dispersion region as pump, parametric fluorescence generates spontaneously[12] by the third order nonlinear interaction between the pump light and zero-point energy in vacuum. Then it experiences parametric amplification and forms symmetric MI sidebands on the two sides of the pump wavelength. The sideband with shorter wavelength is called signal band, while the other is idler band. The frequency difference between pump light and peaks of the two sidebands is determined by the phase matching condition of the parametric process:

$$2\gamma P = \Delta\beta, \tag{1}$$

where γ is the fibre nonlinear coefficient, P is the pump power, and their product is the nonlinear phase mismatch between the pump and the signal, idler light. $\Delta\beta = 2\beta_{\rm p} - \beta_{\rm s} - \beta_{\rm i}$ is the linear phase mismatch, where $\beta_{\rm p}, \beta_{\rm s}, \beta_{\rm i}$ are the wave numbers of pump, signal, and idler lights, respectively. By measurements of frequency differences between pump light and peaks of the two sidebands under different pump wavelengths, the dispersion parameters of the HNMF can be calculated by numerical fitting using the phase matching condition.

The experimented setup for the measurement is shown in Fig.1. The HNMF (fabricated by Crystal fibre A/S Inc) under test is 25m long, which has triangular air hole array structure. Diameters of the silica core and the air holes are 1.8nm and 0.89nm, respectively. The scanning electron microscope image of the cross section is shown in the inset of Fig.1. Its ZDW is about 1565nm (given by the manufacturer) and the total loss is 5.5dB including splice loss at both ends. Its nonlinear coupling coefficient is 66.7/W/km at both axes referring to our previous work.[10] The output light of a tunable external cavity laser (ECL) is modulated by a $LiNiO_3$ modulator (MOD), then amplified by an erbium-doped fibre amplifier (EDFA) to achieve high power pulsed pump light with a repetitive frequency of 0.3MHz and pulse width of 13ns. A polarization controller (PC) is used to adjust the polarization of the pump light. A circulator and a fibre Bragg grating (FBG) are used to suppress the amplified spontaneous emission (ASE) of the EDFA. The power of the pump injecting into the HNMF is monitored by an 1:99 coupler, and measured by an oscilloscope (Agilent54833A) with a photon detector (Agilent83440C) after proper attenuation by a variable optical attenuator (VOA). The output spectra of the HNMF are measured by an optical spectrum analyser (OSA, Agilent86142B).

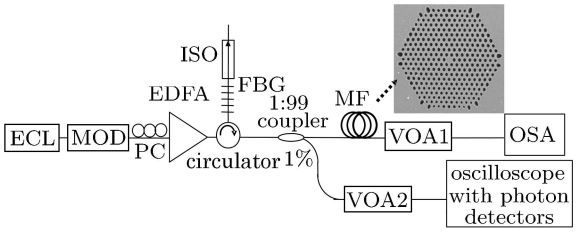


Fig.1. Experimental setup of MI spectrum method for measuring the dispersion parameters.

3. Experimental results

Firstly, the phase birefringence of the HNMF is measured by the white light interference method.[13] The ASE of an EDFA polarized by a polarizer is used as the single polarization white light, which is injected in the HNMF after a PC, then the spectrum is observed by an OSA after another polarizer. Strong interference ripples due to the phase birefringence of the HNMF are presented, which are shown in Fig.2. The ripple period is about 2.8nm, then the phase birefringence about 3.5×10^{-5} can be deduced.

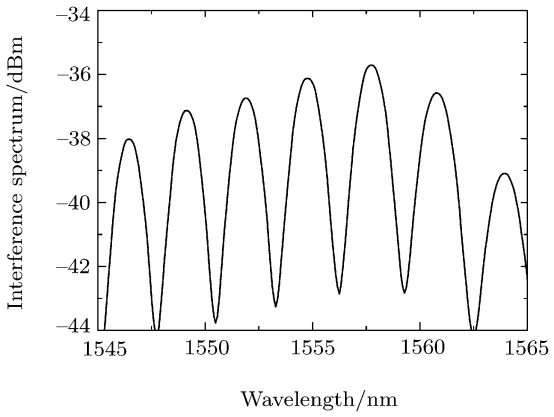


Fig.2. Output spectrum of phase birefringence measurement by the white light interference method.

The dispersion parameters are measured by MI method using the experimental setup in Fig.1. To measure the polarization dependent dispersion properties of the HNMF, the impact of pump polarization on the MI spectrum should be considered. The MI spectrum changes gradually with the changing of pump polarization, showing combined contribution of the pump powers along the two axes. Three typical pump polarization states are used in the measurement, which are along the fast axis, slow axis and 45° from the two axes.

Figure 3 shows the typical MI spectra under different pump polarizations. MI spectra examples when the pump is adjusted to the fast, slow axes and 45° from two principal axes through PC. If the polarization of pump light is adjusted along one of the two principal axes, the MI sidebands are generated in the same axis. The process is called co-polarization MI. It can be seen that the peak values of the co-polarization MI sidebands along the two axes are almost the same, however, the frequency detunings of the sideband peaks are different, shown the impact of polarization dependent GVDs. If the pump polarization departs from the principal axes, the MI spectrum declines sharply as the dash line shows. Beside the co-polarization MI sidebands along the two axes, a pair of small sidebands appears near the pump wavelength due to the cross-polarization[14] MI process, in which pump photons along both axes participate in the cross-polarization MI process, and generate sidebands along different axes.

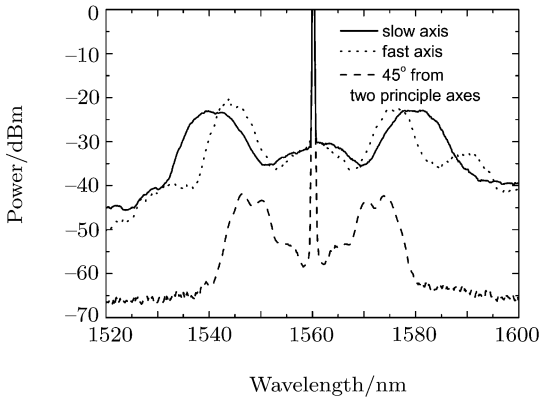


Fig.3. Examples of the MI spectra when the pump is along fast, slow axis or 45° from two principal axes.

3.1. Polarization dependent GVDs and their slopes

We use the co-polarization MI spectrum to measure the polarization dependent GVDs in the two axes. When the pump wavelength in the anomalous dispersion region is far from the ZDW, the linear phase mismatch in Eq.(1) can be expressed as $\Delta\beta = D_{\rm p}\lambda_{\rm p}^2/(2\pi c)\Omega^2$[15] by ignoring the contribution of the high order dispersions. $\Omega = \omega_{\rm p} - \omega_{\rm s} = \omega_{\rm i} - \omega_{\rm p}$ is the angular frequency difference of the sideband from the pump, where $\omega_{\rm p}, \omega_{\rm s}, \omega_{\rm i}$ are angular frequencies of pump, signal and idler, respectively. $\lambda_{\rm p}$ is the wavelength of the pump, $D_{\rm p}$ is the GVD parameter along a certain axis at the pump wavelength. Hence, the GVD can be calculated by:

$$D_{\rm p} = 4\pi c\gamma P/\lambda_{\rm p}^2/\Omega_{\rm peak}^2, \tag{2}$$

where $\Omega_{\rm peak}$ is the frequency difference between the sideband peak of the co-polarization MI and the pump, which can be measured on the MI spectrum directly and represents the frequency detuning satisfying the phase matching conditions.

Figure 4 shows the measured GVD of the HNMF along both axes at different pump wavelength. It can be seen that the GVDs along both axes decrease almost linearly with increasing wavelength, while the GVD parameters are different along the two axes. The five groups of measured data at the short wavelength end are linearly fitted to get the dispersion slopes of the two axes which are -0.763ps/nm^2/km and -0.821ps/nm^2/km respectively. The former is for slow axis and the latter for fast axis, referring to Ref.[9], which shows that the ZDW of the fast axis shift to a higher wavelength in HNMF with high birefringence and the ZDW splitting is proportional to the phase birefringence. The ZDWs along two axes are 1563nm and 1564.4nm, respectively. Then the ZDW splitting of the HNMF under test is 1.4nm, which agrees well with the estimated ZDW splitting (1.5nm)

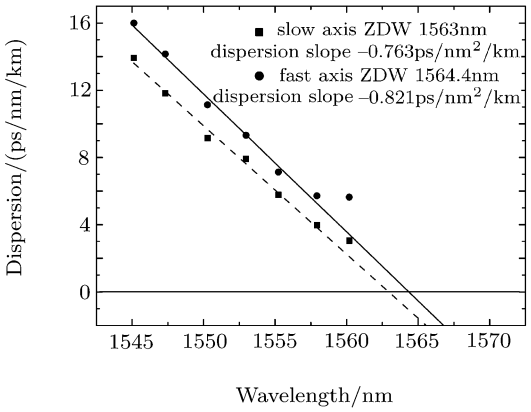


Fig.4. The GVD parameters in two axes.

by the method proposed in Ref.[9], using the measured phase birefringence of the HNMF.

3.2. Fourth-order dispersion

The co-polarization MI spectrum is also used to measure the polarization dependent fourth-order dispersions along the two axes. The calculated GVD parameters in Fig.4 by Eq.(2) are apart from the linear fitting near ZDW, showing that the impact of high-order dispersions should be considered in the phase matching condition of the MI process when the GVD is small. Considering the contribution of the fourth-order dispersion in the linear phase mismatch in Eq.(1), we can write the phase matching condition as

$$D_{\rm p}\lambda_{\rm p}^2/(2\pi c)\Omega_{\rm peak}^2 - \beta_4/12\Omega_{\rm peak}^4 = 2\gamma P, \qquad (3)$$

where $\beta_4 = \partial\beta^4/\partial\omega^4$ is the fourth-order dispersion parameter of the fibre. We measure the $\Omega_{\rm peak}$ under two different pump powers at $\lambda_{\rm p}$=1560.2nm. The GVD parameters fitted in Section 3.1 are used, which are 3.5ps/nm^2/km and 2.2ps/nm^2/km for the fast and slow axes respectively. Table 1 lists the measured $\Omega_{\rm peak}$ and β_4 for the two axes, which is calculated by Eq.(3) and averaged from the results under different pump powers.

Table 1. Relation of the pump power and phase matched frequency difference along the two axes at $\lambda_{\rm p}$=1560.2nm.

	P_1=6.4W	P_2=8.1W	β_4/(ps^4/m)
$\Omega_{\rm peak,f}/2\pi$	1.71THz	1.92THz	−269
$\Omega_{\rm peak,s}/2\pi$	2.35THz	2.59THz	−54

3.3. Group birefringence

We use cross-polarization MI spectrum to measure the group birefringence, also called group delay difference. The nonlinear phase mismatch is $\gamma(P_{\rm s} + P_{\rm f})$, where $P_{\rm s}, P_{\rm f}$ are the pump powers distributed in slow and fast axes. It can be seen from Fig.3 that although the sideband peaks of cross-polarization MI is lower than those of the co-polarization MI, the cross-polarization MI sidebands could not be covered by the co-polarization MI due to the high birefringence. Hence, the frequency difference between the sideband peak of cross-polarization MI and the pump light, which is denoted by $\Omega'_{\rm peak}$, can be measured from the output spectrum of the HNMF. In the case of our experiment, $\Omega'_{\rm peak}$ is small, the phase matching condition for the cross-polarization MI is

$$\tau\Omega'_{\rm peak} + D_{\rm p}\lambda_{\rm p}^2/(2\pi c)\Omega'^2_{\rm peak} = \gamma(P_{\rm s} + P_{\rm f}), \qquad (4)$$

where $\tau = \partial\beta_{\rm s}/\partial\omega - \partial\beta_{\rm f}/\partial\omega$ is the group delay difference of the two axes in unit fibre length. $D_{\rm p}$ is the average GVD value of the two axes at the pump wavelength. The $\Omega'_{\rm peak}\lambda_{\rm p}^2/2\pi c \sim$ 4nm due to cross-polarization MI in Fig.3 under total pump power of 8W. Hence τ is about 0.158ps/m, calculated by Eq.(4).

4. Effect of polarization dependent dispersion

The measurement in Section 3 indicates that the dispersion characteristics of the HNMF under test have high polarization dependence, which should impact the dispersion sensitive nonlinear processes in the HNMF greatly. To demonstrate the effect of the polarization dependent GVD, high power pump injected into the HNMF near the ZDW under different polarization using the experimental setup of Fig.1, in which the pump light filter (the circulator and FBG) is removed to reduce the pump loss before the HNMF and to add the broadband ASE of the EDFA accompanying the pump.

Figure 5 shows the output spectrum when the polarization state of the pump is adjusted by the PC. The peak power of the pump light is $41W$. When pump light polarized along the fast axis, lobes with symmetric frequency detunings on the two sides of pump light appear as the dotted line indicates. The sidebands are generated by the amplified ASE of the EDFA by the MI gain, whose bandwidth is limited by the comparatively high GVD of the fast axis. Several sidebands far from pump light can also be observed, and the first signal sideband collapses, which are due to the four-wave-mixing effect near the ZDW. When the polarization of pump is gradually changing, the satisfaction of the phase matching condition along both axes is possible, which leads to complicated output spectrum as the dash line shows. When most of the pump is along the slow axis, continuous-wave (CW) SC is observed as the solid line shows, which is generated by the combined effects of MI and Raman soliton self-frequency shift, where MI process breaks the CW light into ultra-short soliton pulses,[16]

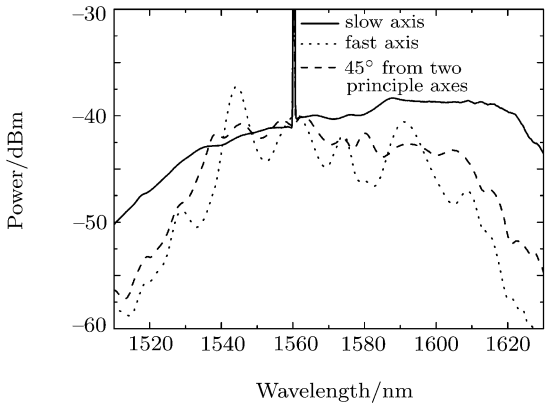


Fig.5. The output spectrum under different pump polarization states.

then the spectra of the pulses shift to longer wavelengths due to intrapulse stimulated Raman scattering. The comparatively low GVD along the slow axis leads to broader MI gain bandwidth, which means that the soliton pulses with short duration and high peak power[17] are more likely to be formed due to the higher modulation frequency of the MI.[18,19] The obvious dependence of the output spectra on the pump polarization shows a clear demonstration of the impact of the polarization dependent dispersion on the nonlinear effects in the HNMF.

5. Conclusion

In this paper, the MI method is used to measure the polarization dependent dispersion of a piece of commercial HNMF, by which the GVD, dispersion slope, the fourth-order dispersion and group birefringence near the ZDW are deduced. A splitting of ZDWs along two axes by 1.4nm is measured. We experimentally demonstrate the impact of the polarization dependent dispersion on the nonlinear effects in the HNMF by CW SC generation. On one axis, MI sidebands with symmetric frequency detunings can be observed, while on the other axis with larger MI frequency detuning, SC is generated by soliton self-frequency shift. The results in this paper indicate that the polarization dependent dispersion properties of HNMFs should be considered seriously in their applications of fibre nonlinear optics.

References

[1] Knight J C, Birks T A, Russell P St J and Atkin D M 1996 *Opt. Lett.* **21** 1547
[2] Zhang Y N, Miao R C, Ren L Y, Wang H Y, Wang L L and Zhao W 2007 *Chin. Phys.* **16** 1719
[3] Knight J C, Arriaga J, Birks T A, Ortigosa-Blanch A, Wadsworth W J and Russell P St J 2000 *IEEE Photon. Technol. Lett.* **12** 807
[4] Ranka J K, Windeler R S and Stentz A J 2000 *Opt. Lett.* **25** 25
[5] Li S G, Ji Y L, Zhou G Y, Hou L T, Wang Q Y, Hu M L, Li Y F, Wei Z Y, Zhang J and Liu X D 2004 *Acta Phys. Sin.* **53** 478 (in Chinese)
[6] Alibart O, Fulconis J, Wong G K L, Murdoch S G, Wadsworth W J and Rarity J G 2006 *New J. Phys.* **8** 67
[7] Wabnitz S 2006 *J. Lightwave Technol.* **24** 1732
[8] Chow K K, Shu C, Lin C and Bjarklev A 2005 *IEEE Photon. Technol. Lett.* **17** 624
[9] Hansen K P, Petersson A, Folkenberg J R, Albertsen M and Bjarklev A 2004 *Opt. Lett.* **29** 14
[10] Zhang W, Xiao L, Zhang L, Huang Y and Peng J 2006 *Chin. Phys. Lett.* **23** 1201
[11] Fatome J, Pitois S and Millot G 2006 *Opt. Fib. Tech.* **12** 243
[12] Ni Y, Wang Q, Liu X, Peng J and Zhou B 2004 *Appl. Phys. Lett.* **85** 3384
[13] Poole C D and Favin D L 1994 *J. Lightwave Technol.* **12** 917
[14] Zhong X Q and Xiang A P 2007 *Chin. Phys.* **16** 1683
[15] Marhic M E, Kagi N, Chiang T K and Kazovsky L G 1996 *Opt. Lett.* **21** 573
[16] Agrawal G P 1995 *Nonlinear Fiber Optics* 2nd edn. (San Diego, CA: Academic)
[17] Tang Y and Yan X H 2000 *Chin. Phys.* **9** 565
[18] Abeeluck A K and Headley C 2005 *Opt. Lett.* **30** 61
[19] Mitschke F M and Mollenauer L F 1986 *Opt. Lett.* **11** 659